Journal of Hazardous Materials 196 (2011) 270–277

Contents lists available at SciVerse ScienceDirect

Journal of Hazardous Materials

journal homepage: www.elsevier.com/locate/jhazmat

Amphiphilic hollow carbonaceous microspheres for the sorption of phenol from water

Zhengrong Guan, Li Liu, Lilu He, Sen Yang*

College of Resources and Environmental Sciences, Biomass Engineering Center, China Agricultural University, Beijing 100193, People's Republic of China

ARTICLE INFO

Article history:
Received 29 June 2011
Received in revised form 19 August 2011
Accepted 7 September 2011
Available online 14 September 2011

Keywords:
Carbonaceous spheres
Removal
Partition
Phenol

ABSTRACT

Amphiphilic porous hollow carbonaceous spheres (PHCSs) were synthesized via mild hydrothermal treatment of yeast cells and further pyrolyzing post treatment. The morphology, chemical composition, porosity, and structure of the carbonaceous materials were investigated. It is evident that the carbonaceous materials were composed of the carbonized organic matter (COM) and the noncarbonized organic matter (NOM), and the relative COM and NOM fractions could be adjusted through changing the temperature of hydrothermal and/or pyrolyzing treatment. The phenol sorption properties of the carbonaceous materials had been investigated and the sorption isotherms fit well to the modified Freundlich equation. It was found that the sorption isotherm of phenol onto PHCSs was practically linear even at extreme high concentrations, which was fewer reported for activated carbon or other inorganic materials. This type of sorption isothermals was assigned to a partition mechanism, and the largest value of the partition coefficient (K_f) and carbon-normalized K_f (K_{oc}) is 56.7 and 91.5 mL g^{-1}, respectively. Moreover, PHCSs exhibit fast sorption kinetic and facile regeneration property. The results indicate PHCSs are potential effective sorbents for removal of undesirable organic chemicals in wastewater, especially at high concentrations.

1. Introduction

Phenol-like compounds have attracted global concerns because of their toxicity and the frequency and quantity of their presence in wastewaters of various industries, such as refineries (6–500 mg L^{-1}), coking operations (28–3900 mg L^{-1}), coal processing (9–6800 mg L^{-1}), and manufacture of petrochemicals (2.8–1220 mg L^{-1}) [1–4]. Phenol-containing wastewater usually involves multiple, different contaminants and the concentration is different from low-concentration of several mg L^{-1} to high-concentration of several thousands mg L^{-1}. Those meanings the best abatement technologies for phenol from wastewaters to be applied strongly depends on single cases, in particular on the concentration of phenol in the stream, the co-presence of other contaminants, the nature of the plant where this problem is found [2]. Now, a number of strategies such as oxidation with ozone/hydrogen peroxide [5], biological methods [6,7], membrane filtration [8], ion exchange [9], electrochemical oxidation [10], photocatalytic degradation [11], and adsorption [12] have been used for the removal of phenol. Review on available technologies for phenol removal from fluid streams has been recently published providing comparison of the experimental conditions and the performances of different techniques [2]. Adsorption is generally considered an operationally simple, effective and widely used process for the removal and recovery of the phenol. Among vast number of different adsorbents, activated carbon (AC) is the most commonly used adsorbent in industrial scale and experimental research [1]. However, AC is not an ideal adsorbent for practical applications at high phenol concentrations, since the adsorption amount of AC will soon saturate. The demanding regeneration and poor mechanical rigidity of AC are also problems for its wider application [13]. Consequently, a large variety of non-conventional adsorbents have been studied for removal of phenol and phenolic pollutants including organoclay [14], polymer [13], carbon nanotube [15], sewage sludge-based adsorbents [16] and activated carbon cloth [17]. However, development of novel adsorbent materials for removal and recovery of the phenol and phenolic pollutants with high concentrations still remains an important challenge.

Yeast, a by-product of the brewing industry, is considered as an industrial organic waste that causes a great deal of concern [18]. In a previous study, we reported a facile method for fabricating porous hollow carbonaceous spheres (PHCSs) with controlled shell porosity from *Saccharomyces cerevisiae* (*S. cerevisiae*) cells [19,20]. Through mild hydrothermal treatment of these tiny unicellular organisms, hollow microspheres with controllable meso- and macroporous shells were synthesized. Most interestingly, the surfaces of these hollow spheres were found to be covered with both hydrophobic and hydrophilic functional groups, endowing the as-obtained microspheres with amphiphilic property. Actually, we found that PHCSs could be well dispersed not only in water but also

* Corresponding author. Tel.: +86 10 62733470; fax: +86 10 62733470.
E-mail address: syang@cau.edu.cn (S. Yang).

0304-3894/$ – see front matter © 2011 Elsevier B.V. All rights reserved.
doi:10.1016/j.jhazmat.2011.09.025

in nonpolar solvents such as toluene and chloroform. This inspired us to speculate that PHCSs may be promising sorbent for organic pollutant from aqueous solution. Herein, four kinds of PHCSs were synthesized via mild hydrothermal treatment of yeast cells and further pyrolyzing post treatment. And the morphology, chemical composition, porosity, and structure of the carbonaceous materials were investigated. The sorption behavior (i.e., sorption isotherms, kinetics models, and the influence of pH and temperature) of PHCSs toward phenol was examined. The relationship existing between the specific surface area and the chemical composition of PHCSs and their phenol sorption capability was elucidated. Lastly, principal sorption mechanisms were clarified.

2. Experimental

2.1. Synthesis of PHCS

PHCSs were synthesized via mild hydrothermal treatment of yeast cells using modified methods described in our previous studies [19]. Typically, *S. cerevisiae* cells (3–4 g, purchased from Angel Yeast Co., Ltd., China) pre-washed with acetone were dispersed in 2–3% (v/v) glutaraldehyde and diluted (less than 0.01 mol L^{-1}) nitric acid aqueous solution (40 mL), which was then placed in a 50 mL Teflon-sealed autoclave and maintained at 180 or 230 °C for 8 h. The puce solid products were centrifugal separated, then washed by three cycles of centrifugation/washing/redispersion in deionized water and alcohol, and oven-dried at 80 °C for 4 h. The PHCSs samples hydrothermally treated at 180 and 230 °C were denoted as P180 and P230, respectively. The samples denoted as P350 and P700 were prepared via further pyrolyzing P180 at temperature of 350 °C and 700 °C for 1 h, respectively, by a tubular reactor in a flow of nitrogen (15 mL min^{-1}).

2.2. Characterization of PHCS

The morphology of the materials was inspected with a field emission scanning electron microscope (SEM, JEOL, JSM-6700F, Japan). Surface area and pore volume of the materials were measured by N_2 adsorption/desorption isotherms at 77 K with a Physisorption Analyzer (Micromeritics, ASAP 2020, U.S.A.). Fourier-transform infrared (FTIR) analysis was performed by a Micro FTIR spectrometer (Nicolet, Magna 750 Nic-Plan FTIR Microscope, U.S.A.) in the spectral region of 4000–650 cm^{-1}. Solid-state cross-polarization magic angle-spinning and total-sideband-suppression ^{13}Carbon nuclear magnetic resonance (^{13}C NMR) spectrum (CPMAS-TOSS) were obtained by a Bruker Avance 400 MHz spectrometer (Karlsruhe, Germany). The C, H, N, O contents of the samples were determined using elemental analyzer (Elementar, Vario EL, Germany). The atomic ratio of (O + N)/C, O/C, H/C were calculated with the element content.

2.3. Sorption experiments

Batch experiments were carried out using a series of 15 mL screw cap centrifuge tube covered with Teflon sheets to prevent the introduction of any foreign particle contamination. In typical batch experiment, 20 mg of the sorbent was added to 10 mL phenol solution at various concentrations (0–10,000 mg L^{-1}) taken in sealed tubes, which were placed in the thermostat shaking assembly. The solutions were shaken at 150 rpm and constant temperatures for 24 h to achieve equilibration. After equilibrium, the mixtures were filtrated through 0.45 μm nitrocellulose syringe filters. The phenol concentrations in the filtrates were determined by a UV-visible spectrometer (Persee, TU-1810, China) at the maximum adsorption wavelength of phenol (270 nm) and pH 6 (pH adjusted with 0.5 M HCl or NaOH). Isotherms were performed by taking different concentrations of phenol at designed temperatures and pH values. All the experiments were carried in triplicate and the averaged data were reported. Standard deviations were found to be within 2.0%. Furthermore, the error bars for the figures were smaller than the symbols used to plot the graphs and hence are not shown in the figures.

2.4. Sorption models and statistical analysis

Freundlich model was applied for sorption data fitting in this work due mainly to its advantages in isotherm nonlinearity investigation. To facilitate direct comparisons of sorption affinities among the samples tested, and investigate the effect of temperature on sorption, the modified Freundlich equation was applied for sorption data fitting in this work:

$$\log\ q_e = \log K'_F + n \log C_r \quad (1)$$

$$C_r = \frac{C_e}{S_w} \quad (2)$$

where q_e is the solid-phase concentration (mg g^{-1}), C_e is the liquid-phase equilibrium concentration (mg L^{-1}); S_w is the solubility of phenol for a given temperature (mg L^{-1}) and C_r is dimensionless since the value of S_w is constant for a given temperature and is expressed in the same unit as C_e; K'_F and n are the modified Freundlich adsorption parameters, K'_F (mg g^{-1}) is the sorption capacity coefficient, which represents the mass of phenol sorbed per unit mass of sorbent when the C_e concentration approaches saturation, and n (dimensionless) is an indicator of isotherm nonlinearity related to the heterogeneity of sorption sites[21].

The partition–adsorption model for describing sorption from aqueous solutions on heterogeneous solids was also analyzed [14,22]:

$$Q_T = Q_A + Q_P \quad (3)$$

where Q_T is the total amount of phenol sorbed onto the sorbent; Q_A and Q_P are the amounts contributed by adsorption and partition, respectively.

According to the partition–adsorption model, the partition effect is favored progressively by increasing the solute concentration, whereas the adsorption contribution reaches saturation more rapidly with the solute concentration. The isotherm at high concentrations should approach linearity. Therefore, at the high solute concentration range the adsorption becomes saturation and the linear partition remains. Thus, Eq. (3) can be transformed to:

$$Q_T = Q_A^{max} + Q_P = Q_A^{max} + K_f C_e \quad (4)$$

$$K_{oc} = \frac{K_f}{f_{oc}} \quad (5)$$

where Q_A^{max} is the saturated adsorption capacity estimated from the high concentration data; $K_f C_e$ is the partition contribution at high concentration with K_f being the partition coefficient; C_e is the solute equilibrium concentration (mg L^{-1}); K_{oc} is carbon-normalized K_f, and f_{oc} is the percentage of carbon contents of sorbent. Linear regression between Q_T and C_e were conducted at high solute concentration range, and the Q_A^{max} corresponds to the y-axis intercept of the line, and K_f to the slope.

2.5. Sorption kinetics

For kinetic studies the batch technique was used. Typically, 20 mg of PHCSs were added 10 mL phenol solution (2000 mg L^{-1}) into series of screw cap centrifuge tubes, and then shaken in constant temperature rotary shaker (150 rpm) at 25 ± 0.5 °C. The

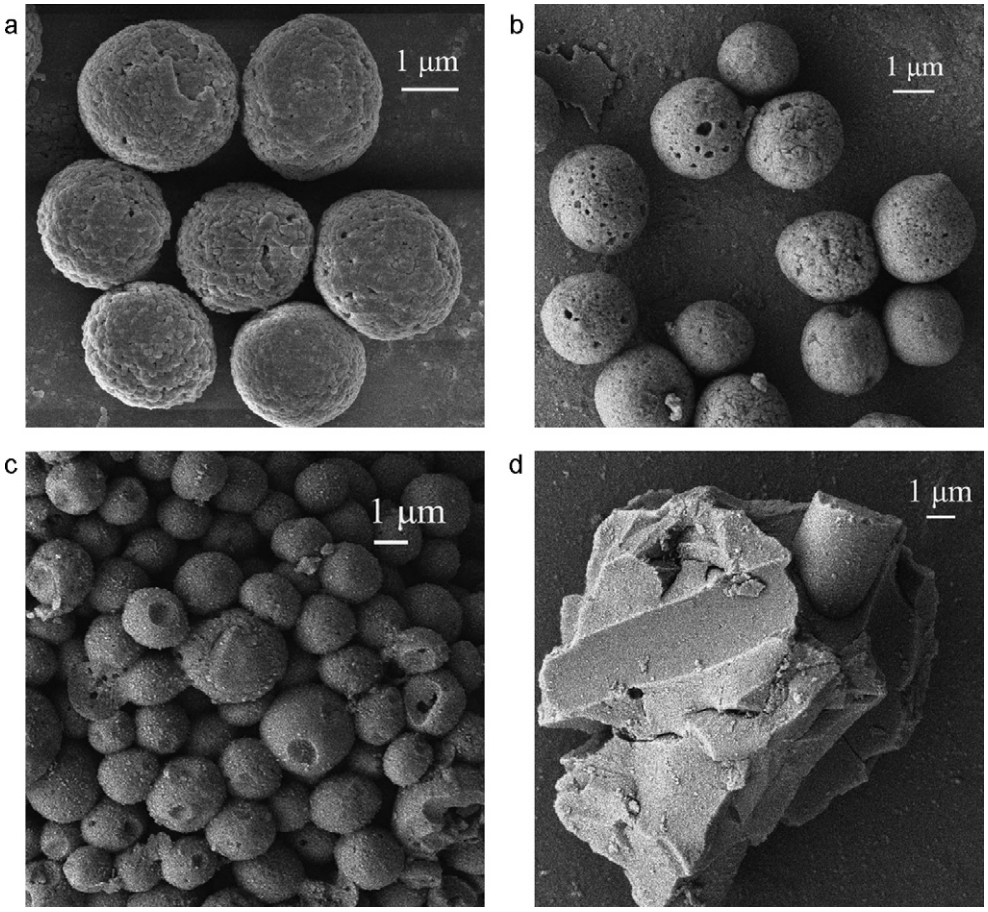

Fig. 1. SEM images of (a) P180, (b) P230, (c) P350 and (d) P700.

concentrations of phenol in solution were sampled and analyzed with different time intervals, and the averaged data were reported.

Linear pseudo-first and pseudo-second order models were given in the following equations [23,24]:

$$\ln(q_e - q_t) = \ln\ q_e - k_1 t \tag{6}$$

$$\frac{t}{q_t} = \frac{1}{k_2 q_e^2} + \frac{t}{q_e} \tag{7}$$

$$t_{1/2} = \frac{1}{k_2 q_e} \tag{8}$$

$$h = k_2 q_e^2 \tag{9}$$

where q_e and q_t (both in mg g^{-1}) are the amount of phenol sorbed on per unit mass of sorbent at equilibrium and at time t (h), respectively; k_1 (h^{-1}) and k_2 (g mg^{-1} h^{-1}) are the pseudo-first-order and pseudo-second-order rate constants, respectively. Moreover, for the pseudo-second-order kinetic model, the half sorption time ($t_{1/2}$) and the initial sorption rate (h) are given (Eqs. (8) and (9)). The value of $t_{1/2}$ is the time required to uptake half of the maximal sorbed amount of sorbate at equilibrium.

3. Results and discussion

3.1. Characterization of PHCSs

SEM images and optical microscopy photos of the carbonaceous products are shown in Figs. 1 and S1, respectively. It was found that the hydrothermal products (P180 and P230) were porous hollow microspheres in the size range 2.0–4.0 μm, which was consistent with our previous results [19]. The thermal stability of the microspheres was satisfactory. After post pyrolyzing treatment of P180 at 350 °C, the microsphere structure was still well preserved (Fig. 1c for P350). Further increasing the pyrolyzing treatment temperature to 700 °C, however, the morphology of materials changed from microspheres into larger carbon blocks (Fig. 1d for P700). Surface area and pore volume of the materials were measured by N_2 adsorption/desorption isotherms at 77 K and all the BET surface areas of the materials are below 10 m^2 g^{-1} (Table 1). N_2 adsorption/desorption isotherm of the materials at 77 K with corresponding pore size distributions are shown in Fig. S2.

Fig. 2 shows the solid-state ^{13}C NMR spectra of the carbonaceous products. Peaks at δ = 26 and 31 ppm can be attributed to methyl and methylene, respectively, and those in the δ = 120–150 ppm region can be assigned to long-range conjugated C=C bonds and oxygen-substituted C=C bonds, revealing the existence of aromatic furan ring compounds [25,26]. Moreover, oxygenated functional groups, including carbonyl, carboxy, hydroxy, ether, and ester groups were also detected. The content of aromatic species was enhanced remarkably by pyrolyzing treatment of the hydrothermal products, indicating high carbonization degree for P350 and especially P700. Moreover, the average chemical shift decreases with the sequence of the carbonization, resembling to some extent the resonance pattern of graphite. Corresponding Fourier transform infrared (FTIR) spectra of the carbonaceous materials are shown in Fig. 3. Both aliphatic and aromatic species were revealed for P180, P230 and P350. The bands at 2925, 2861, 1442, and 1372 cm^{-1} are assigned mainly to CH_2 units [27]. Those at 1693 and 1160 cm^{-1} are assigned to C=O and C–O stretching vibrations of ester bonds, respectively. And the band at 1602 cm^{-1} is assigned to C=C and C=O

Table 1
Elemental compositions, atomic ratios, BET surface area (SA), and total pore volume (TPV) of the carbonaceous materials.

Sample	Treatment temperature (°C)	C (wt.%)	H (wt.%)	O (wt.%)	N (wt.%)	(O + N)/C ratio	O/C ratio	H/C ratio	SA ($m^2\ g^{-1}$)	TPV ($mL\ g^{-1}$)
P180	180	62.00	6.25	21.16	6.08	0.34	0.26	1.21	9.504	0.0498
P230	230	72.96	6.99	12.15	4.88	0.18	0.13	1.14	2.635	0.0095
P350	350	73.22	4.44	10.61	6.27	0.18	0.11	0.72	1.960	0.0052
P700	700	77.17	1.94	5.71	5.06	0.11	0.06	0.30	2.830	0.0080

H/C: atomic ratio of hydrogen to carbon. O/C: atomic ratio of oxygen to carbon. (O + N)/C: atomic ratio of sum of nitrogen and oxygen to carbon.

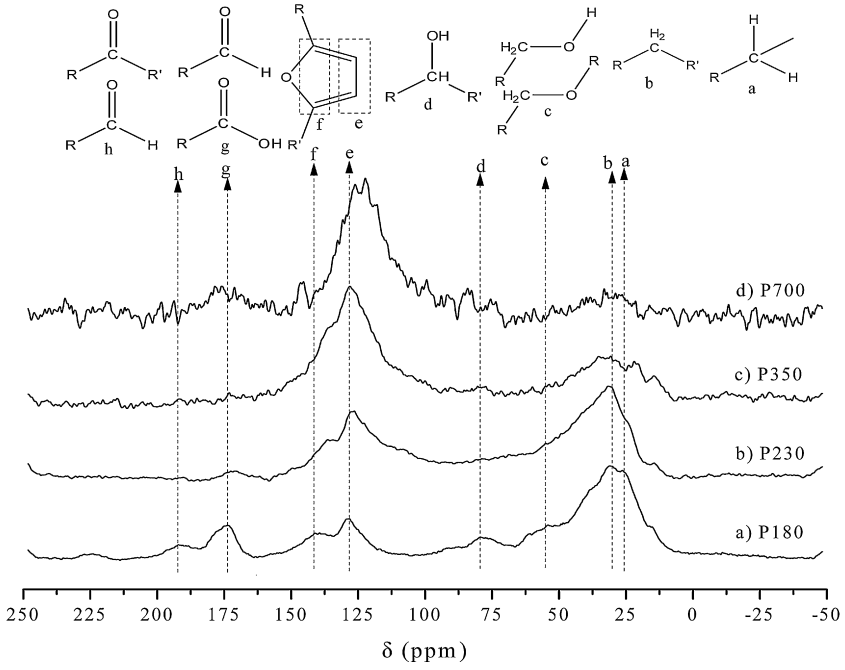

Fig. 2. Solid-state ^{13}C NMR spectrum of (a) P180, (b) P230, (c) P350 and (d) P700.

stretching in the aromatic ring [22]. The peak of 786, 706 cm^{-1} can be assigned to the aromatic CH out-of-plane deformation. In the case of P700, almost all of the band intensities mentioned above are dramatically decreased or disappeared, indicating destruction of the surface function groups and chemical structure after pyrolyzing treatment at high temperatures.

The elemental compositions shown in Table 1 agree well with the observations of FTIR. O content decreased from 21.16% for

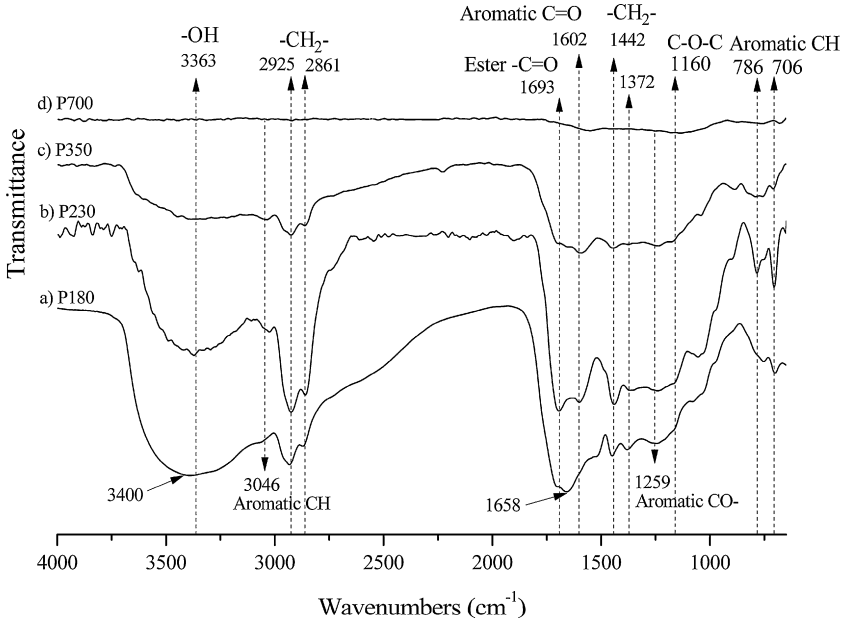

Fig. 3. FTIR spectrum of (a) P180, (b) P230, (c) P350 and (d) P700.

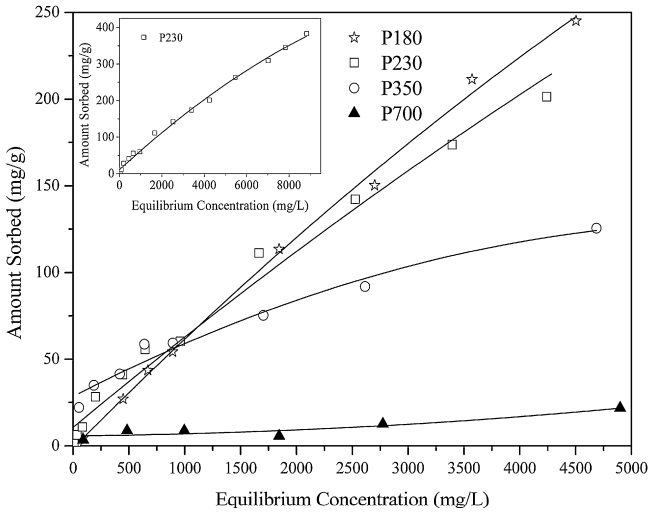

Fig. 4. Sorption isotherms of phenol on carbonaceous products in aqueous solution at 25 °C and pH 6, inset: sorption isotherms on P230 at high phenol concentrations.

P180 to 12.15% for P230 and further declined slightly to 10.61% for P350. When the pyrolyzing treatment temperature was increased to 700 °C, the O content declined drastically to 5.71% (P700). The H content of P350 and P700 declined dramatically from about 6.25% (P180) to 4.44% and 1.94%, respectively. These results mean that the degree of carbonation of samples increased with higher hydrothermal and pyrolyzing temperature. The H/C ratio and O/C ratio decreases with deep carbonization, indicating the surfaces of the products become less hydrophilic [28]. The decrease of the polarity index [(O + N)/C] with the degree of carbonization reveals a reduction of the surface polar functional groups [22].

All the above results reveal that both hydrothermal and pyrolyzing treatment changed the chemical composition of PHCSs to a large degree. Due to the partial loss of the hydrophilic groups and aromatization of the molecule networks, wettability characteristics of PHCSs were supposed to be very different from that of the original hydrophilic yeast cells. We found all samples except P700 could be well dispersed not only in water but also in nonpolar solvents (Fig. S3), suggesting that PHCSs possess amphiphilic surfaces, as we reported previously [19,20]. Moreover, there are two types carbon species in the PHCSs, namely alkyl carbon and aromatic carbon. The alkyl carbon is mainly derived form the noncarbonized organic matter (NOM) of the yeast cells, and the aromatic carbon is the products of carbonization, i.e., the carbonized organic matter (COM). It is evident that the relative COM and NOM fractions could be adjusted through changing the temperature of hydrothermal and/or pyrolyzing treatment. While there are large amounts of NOM in the samples of P180, P230 and P350, COM is dominant in P700. The amphiphilic property and the specific chemical composition of the PHCSs make them may be excellent potential sorbents for organic compounds removal from wastewater. Subsequently, the sorption isotherms of phenol were carried out.

3.2. Sorption isotherms

Sorption of phenol onto the carbonaceous materials at 25 °C was investigated and the results are presented in Fig. 4. The sorption of P700 was saturated at very low phenol concentration (86 mg L^{-1}) and the sorption amount was only 5.5 mg g^{-1}, which may be due to the very low surface area (2.8 m^2 g^{-1}). Because P700 was produced by pyrolyzing P180 at 700 °C for 1 h, the high carbonization degree and few surface function groups (Figs. 2 and 3) suggested that the sorption mechanism of P700 is physical adsorption.

The result means P700 cannot be used as sorbents for organic compounds, and so we did not discuss about P700 any more. The surface area of P180, P230 and P350 was all less than 10 m^2 g^{-1}, however, they exhibited quite different sorption behaviors: surface area-independent sorption amount and the almost linear isotherm without a saturated sorption. This sorption characteristic was fewer reported for AC [29,30] or other inorganic adsorbent materials [31], which suggests that the sorption mechanism of PHCSs is not simple physical or chemical adsorption.

Modified Freundlich model was applied to investigate the isotherm nonlinearity of PHCSs. The sorption isotherms fit well to the modified Freundlich equation and the calculated parameters are listed in Table 2. The isotherm of phenol onto P180 is practically linear, with Freundlich $n = 1.016 \pm 0.025$, and the isotherms for P230 and P350 display different nonlinearity of a concave-downward curvature at low solute concentrations but exhibit a practically linear shape at moderate to high concentrations. The nonlinear effects are relatively more visible for the P350 than for the P230. Similar results were observed for sorption of organic solutes from water over a wide range of C_e/S_w by black carbons (BCs) or biochars, derived mainly from the incomplete combustion of biomass and fossil fuel [22,32,33]. The unique isotherm shape, i.e., nonlinear at low C_e/S_w but virtually linear at other C_e/S_w, suggests that more than a single mechanism be operative over the entire concentration range [34]. To explain the nonlinearity of sorption isotherms, dual-mode sorption models (DMSM) or dual-reactive domain models (DRDM) were suggested. According to these models [14,22,32,33,35], the sorbent was considered to be a heterogeneous substance, and a concept of NOM (or "soft carbon", expanded, rubbery state) vs. COM (or "hard carbon", condensed, glassy state) was been invoked to operationally delineate chemical heterogeneity of sorbent and to elucidate the mechanisms for sorption by soils, sediments, biochars and charcoal. The COM is expected to behave as an physical adsorbent, producing isotherm nonlinearity, and the NOM can uptake pollutants via a partition (sorption) mechanism [22,32,33]. One unique feature of the partition process is that the ratio of solid phase to aqueous-phase concentrations remains unchanged with the variation of the solute concentration. In this sense, the sorptive uptakes are determined by the relative carbonized and noncarbonized fractions and their surface and bulk properties. Thus, the linearity of P180 can be assigned to sorption of phenol to NOM via partition mechanism, since NOM is the mainly carbon species in this sample. The nonlinearity of P230 and P350 at low C_e/S_w is attributed to a combined physical adsorption on a small amount of COM and a partition effect of NOM. At moderate to high C_e/S_w, the physical adsorption becomes largely saturated and the partition in NOM predominates to give an essentially linear isotherm. The larger curvature at low C_e/S_w of P350 is presumably due to the higher content of aromatic moieties with increased carbonization degree. The adsorption behavior of P700 with highest carbonization degree, validate this speculation. High isotherm nonlinearity was also observed for high-temperature chars [33].

From the partition–adsorption model, Q_A^{max}, K_f and K_{oc} were calculated (Table 2), The K_f and K_{oc} increase in the order of P350 < P230 < P180, which is in inverse with their carbonization degree. The physicochemical nature of the organic carbon has been suggested as a major factor controlling sorption of organic compounds to natural or modified organic sorbent. According to FTIR and NMR data (Figs. 2 and 3), the major partition phase in P180, P230 and P350 is a polymeric aliphatic fraction preserved during the hydrothermal process, and the content of aliphatic fraction increased in the order of P350< P230 < P180, which is in the line with the increased partition effect. The similar conclusions were also presented by other researchers [22,36]. Chefetz et al. [36] tested the sorption of pyrene to a series of sorbents comprised of different levels of aromaticity and aliphaticity. In that study, a

Table 2
Modified Freundlich model parameters, partition coefficients and saturated adsorption of phenol to PHCs.

Sample	Modified Freundlich model parameters			Partition–adsorption model		K_{oc} (mL g^{-1})	$Q_{A,SA}^{max}$ (mg g^{-1} m^{-2})
	log K_F [a]	n [b]	R^2	K_f (mL g^{-1})[c]	Q_A^{max} (mg g^{-1})[c]		
P180	3.733 ± 0.049	1.016 ± 0.025	0.996	56.7	0	91.5	0
P230[d]	3.102 ± 0.024[d]	0.661 ± 0.013[d]	0.997[d]	25.8[d]	67.3[d]	35.4[d]	25.5
P230	3.434 ± 0.058	0.822 ± 0.025	0.987	38.2	45.8	52.5	17.4
P230[e]	3.230 ± 0.018[e]	0.700 ± 0.009[e]	0.991[e]	39.4[e]	34.3[e]	54.0[e]	13.0
P350	2.543 ± 0.041	0.378 ± 0.019	0.986	17.3	45.15	23.6	23.0

K_{oc} is carbon-normalized K_f. $Q_{A,SA}^{max}$ is the SA-normalized Q_A^{max}. The solubility of phenol in water at 15, 25 and 35 °C is 8200 mg/100 mg, 8660 mg/100 mg and 9910 mg/100 mg, respectively.

[a] 95% confidence interval of log K_F.
[b] 95% confidence interval on n.
[c] The slope and y-axis intercept of the linear equation were used to calculate partition coefficient (K_f) and the maximum adsorption capacity (Q_A^{max}, mg g^{-1}, Chen et al. [22]), respectively.
[d] Tested at 15 °C.
[e] Tested at 35 °C.

positive trend was observed between the K_{oc} level and the aliphaticity of the set of samples. Chen et al. [22] performed sorption experiments with biochars, produced by pyrolysis of pine needles at different temperatures. This study clearly demonstrated that a greater sorption affinity of naphthalene, nitrobenzene, and m-dinitrobenzene with aliphatic-rich biochars than with aromatic-rich biochars.

The $Q_{A,SA}^{max}$ of P230 and P350 was listed in Table 2, which exceeds greatly the amount accountable by the small surface area of the sorbent. Some researchers also reported the higher adsorption of polar solutes compared with the little sorbent surface area. To explain the higher sorption of polar pesticides at low (relative) concentrations, Spurlock and Biggar [37] suggested the specific-interaction model. The model postulates that the specific interaction of polar solutes with highly active sites of organic carbon phase. That implies that more highly active site, more specific interaction, and higher $Q_{A,SA}^{max}$. P350 showed less oxygen content and highly active site because of pyrolyzed dehydration at 350 °C, however, the $Q_{A,SA}^{max}$ of P350 is 23.0 mg g^{-1} m^{-2}, higher than the 17.4 mg g^{-1} m^{-2} of P230. We speculated the possible phenol–sorbent interaction may be hydrophobic effect since P350 showed higher hydrophobicity compared with P230.

3.3. Sorption kinetics

Fig. 5 shows the sorption kinetics of phenol onto P180 and P230. Apparently, the sorption rates were very fast. For example, given the tested conditions, approximately 86 and 85% of sorption was accomplished within 0.5 h for P180 and P230, respectively. For quantitative comparison of apparent sorption kinetics between P180 and P230, the data were fitted to the pseudo-first order and pseudo-second order models, respectively. The sorption kinetic constants were listed in Table 3. The regression coefficient (R^2) for the pseudo-first order model varied from 0.9830 to 0.7022 and the Q_e values calculated from the model deviated tremendously from the experimental values, together indicating the invalidity of the model. However, the pseudo-second-order model provided the best fitting for the all experimental data. The plots show regression coefficients higher than 0.9997 for P180 and P230. The value of the constant k_2 of P180 is higher than that of P230, which inversely correlates with the K_f. Thus, it could be speculated that kinetics of phenol following the pseudo-second-order model are controlled by an adsorption process and adsorption was the main sorption rate-limiting step.

3.4. Effect of temperature on sorption

To investigate the effect of temperature on the sorption of phenols, sorption experiments were conducted at 15, 25 and 35 °C for P230. The results are shown in Fig. 6. The parameters of

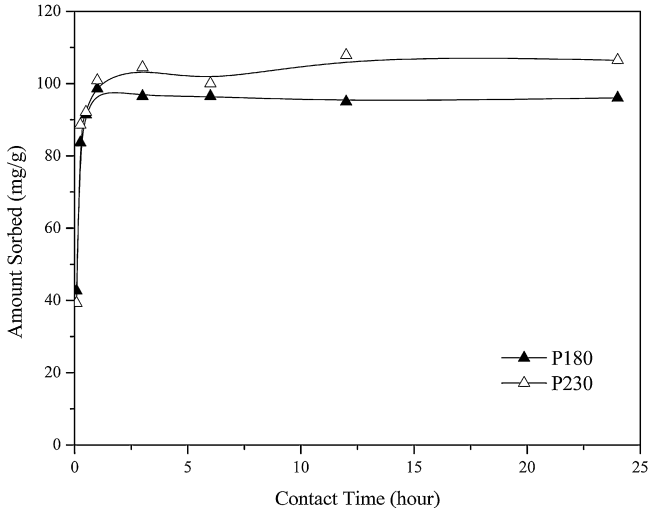

Fig. 5. Sorption kinetics plotted as sorbed amount of phenol vs. time on P180 and P230 with a 2000 mg L^{-1} initial phenol concentration and 25 °C.

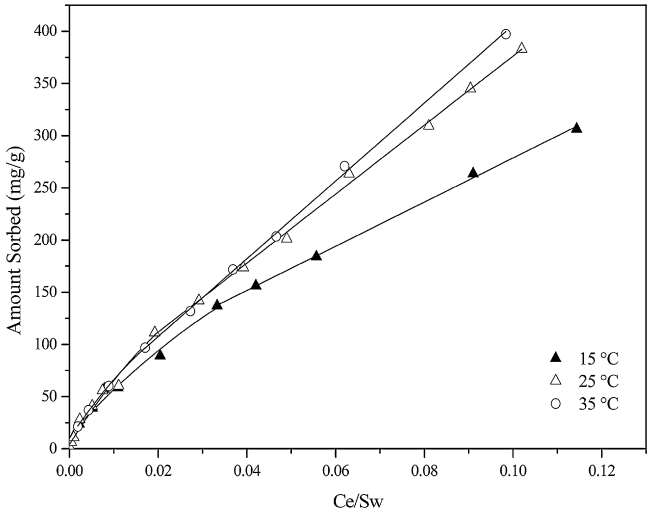

Fig. 6. Sorption isotherms of phenol on P230 at 15, 25 and 35 °C at pH 6.

Table 3
Adsorption rate constants for two kinetic models at 25 °C and pH of 6.

Sample	q_e (exp)[a] (mg g^{-1})	First-order model			Second-order model				
		K_1 (h^{-1})	q_e (cal)[b] (mg g^{-1})	R^2	K_2 (g mg^{-1} h^{-1})	q_e (cal)[b] (mg g^{-1})	$t_{1/2}$ (h)	h (mg g^{-1} h^{-1})	R^2
P180	98.63	3.17	82.92	0.9830	0.1028	110.31	0.099	1000	0.9997
P230	107.85	0.12	19.86	0.7022	0.0660	106.80	0.14	769	0.9998

[a] Experimental data.
[b] Calculated data from models.

modified Freundlich adsorption model and partition–adsorption model are incorporated in Table 2. A comparison of modified Freundlich parameter n shows that the biggest value was got at 25 °C and the smallest value at 15 °C. This means that the effect of temperature on the adsorption and partition is different. Comparing with Q_A^{max} and K_f of P230 at 15, 25 and 35 °C, we can find that partition increase with an increase in temperature, meaning that temperature may play an important role for the partition coefficient K_f. To date, fewer K_f values have been reported for hydrophobic organic contaminants (HOCs) at temperatures other than 25 °C, and the reported conclusion is different [38]. Chen and Pawliszyn [39] evaluated the effect of temperature on K_f for BTEX compounds and found that K_f should not be greatly dependent on temperature. Muijs and Jonker [40] determined K_f values for several PAHs and found that temperature can play a significant role. We speculated that the increasing K_f values of P230 for phenol with increasing temperature maybe due to the polarity of phenol and the structure of P230. However, the adsorption decreases with an increase in temperature indicate that the process is apparently exothermic.

3.5. Effect of pH value on sorption

The effect of pH on the sorption ability of P230 was investigated and the results are shown in Fig. 7. According to the model proposed by Deryło-Marczewska and Marczewski [41], the adsorption of non-ionized compound does not depend on the pH and the surface charge. The sorption isotherms at the pH of 3 and 6 coincided. This may be due to the dissociation degree of phenol is very low (pK_a = 9.89) in acidic conditions. However, the sorption at pH of 11 obviously decreased since phenol is highly dissociated at pH 11 and dissolved into water.

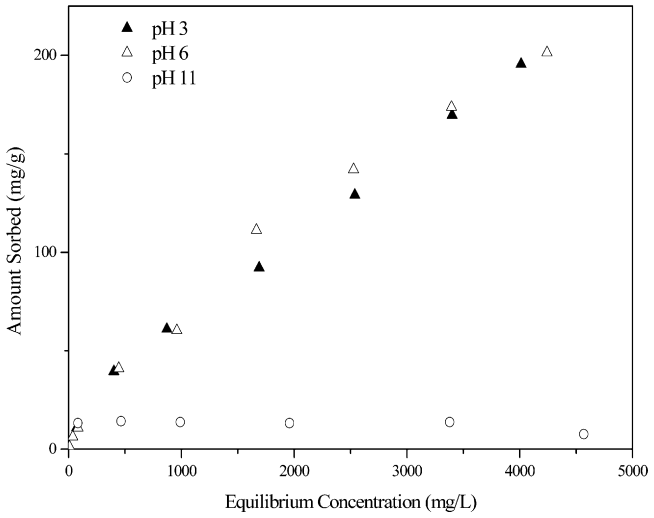

Fig. 7. Sorption isotherms of phenol on P230 at pH 3, 6 and 11 at 25 °C.

3.6. Sorbent regeneration

Important goals in the development of sorbent materials include simple regeneration and sorbate isolation [42]. Regeneration allows for the repeated use of the sorbent material and decreasing costs. It was found that desorption of phenol from the loaded P230 using 0.01 M NaOH solution was rapid. For example, after placing P230 that had sorbed 141 mg g^{-1} phenol in a 0.01 M NaOH solution for 10 min, the regenerated P230 showed greater than 98% of the phenol was removed from the sorbent. The facile regeneration is due to the high solubility of the sodium salt of phenol in water.

4. Conclusions

Amphiphilic PHCSs were synthesized via mild hydrothermal treatment of yeast cells and further pyrolyzing post treatment. The sorption properties of PHCSs for phenol in aqueous solutions were investigated, and then reached the following conclusions:

(1) PHCSs were composed of COM and NOM, and the relative COM and NOM fractions could be adjusted through changing the temperature of hydrothermal and/or pyrolyzing treatment.
(2) The sorption isotherm of phenol onto PHCSs was practically linear even at extreme high concentrations. This type of sorption isothermals was assigned to a partition mechanism, and the largest value of the partition coefficient (K_f) and carbon-normalized K_f (K_{oc}) is 56.7 and 91.5 mL g^{-1}, respectively.
(3) PHCSs exhibit fast sorption kinetic and facile regeneration property.

The results indicate they are potential effective sorbents for removal and recovery of undesirable organic chemicals in water treatment, especially at high concentrations.

Acknowledgments

This work was supported by the National Natural Science Foundation of China (20703065, 20877097, and 20806089), the Ministry of Science and Technology of China (2008AA06Z324) and Chinese Universities Scientific Fund (2011JS160).

Appendix A. Supplementary data

Supplementary data associated with this article can be found, in the online version, at doi:10.1016/j.jhazmat.2011.09.025.

References

[1] M. Ahmaruzzaman, Adsorption of phenolic compounds on low-cost adsorbents: a review, Adv. Colloid Interface Sci. 143 (2008) 48–67.
[2] G. Busca, S. Berardinelli, C. Resini, L. Arrighi, Technologies for the removal of phenol from fluid streams: a short review of recent developments, J. Hazard. Mater. 160 (2008) 265–288.
[3] A. Bahdod, S. El Asri, A. Saoiabi, T. Coradin, A. Laghzizil, Adsorption of phenol from an aqueous solution by selected apatite adsorbents: kinetic process and impact of the surface properties, Water Res. 43 (2009) 313–318.

[4] C.R. Ispas, M.T. Ravalli, A. Steere, S. Andreescu, Multifunctional biomagnetic capsules for easy removal of phenol and bisphenol A, Water Res. 44 (2010) 1961–1969.
[5] O. Chedeville, M. Debaccq, M.F.A. Almanza, C. Porte, Use of an ejector for phenol containing water treatment by ozonation, Sep. Purif. Technol. 57 (2007) 201–208.
[6] G. Annadurai, R.S. Juang, D.J. Lee, Microbiological degradation of phenol using mixed liquors of *Pseudomonas putida* and activated sludge, Waste Manage. 22 (2002) 703–710.
[7] N. Massalha, A. Shaviv, I. Sabbah, Modeling the effect of immobilization of microorganisms on the rate of biodegradation of phenol under inhibitory conditions, Water Res. 44 (2010) 5252–5259.
[8] W. Cichy, J. Szymanowski, Recovery of phenol from aqueous streams in hollow fiber modules, Environ. Sci. Technol. 36 (2002) 2088–2093.
[9] Z.M. Ahmed, S. Lyne, R. Shahrabani, Removal and recovery of phenol from phenolic wastewater via ion exchange and polymeric resins, Environ. Eng. Sci. 17 (2000) 245–255.
[10] L.Z. Wang, Y.M. Zhao, J.F. Fu, The influence of TiO_2 and aeration on the kinetics of electrochemical oxidation of phenol in packed bed reactor, J. Hazard. Mater. 160 (2008) 608–613.
[11] R. Vinu, G. Madras, Kinetics of simultaneous photocatalytic degradation of phenolic compounds and reduction of metal ions with nano-TiO_2, Environ. Sci. Technol. 42 (2008) 913–919.
[12] F.A. Banat, B. Al-Bashir, S. Al-Asheh, O. Hayajneh, Adsorption of phenol by bentonite, Environ. Pollut. 107 (2000) 391–398.
[13] B.C. Pan, W. Du, W.M. Zhang, X. Zhang, Q.R. Zhang, B.J. Pan, L. Lv, Q.X. Zhang, J.L. Chen, Improved adsorption of 4-nitrophenol onto a novel hyper-cross-linked polymer, Environ. Sci. Technol. 41 (2007) 5057–5062.
[14] L.Z. Zhu, B.L. Chen, X.Y. Shen, Sorption of phenol, p-nitrophenol, and aniline to dual-cation organobentonites from water, Environ. Sci. Technol. 34 (2000) 468–475.
[15] D.H. Lin, B.S. Xing, Adsorption of phenolic compounds by carbon nanotubes: role of aromaticity and substitution of hydroxyl groups, Environ. Sci. Technol. 42 (2008) 7254–7259.
[16] K.M. Smith, G.D. Fowler, S. Pullket, N.J.D. Graham, Sewage sludge-based adsorbents: a review of their production, properties and use in water treatment applications, Water Res. 43 (2009) 2569–2594.
[17] E. Ayranci, O. Duman, Adsorption behaviors of some phenolic compounds onto high specific area activated carbon cloth, J. Hazard. Mater. 124 (2005) 125–132.
[18] W. Lamoolphak, M. Goto, M. Sasaki, M. Suphantharika, C. Wangnapoh, C. Prommuag, A. Shotipruk, Hydrothermal decomposition of yeast cells for production of proteins and amino acids, J. Hazard. Mater. 137 (2006) 1643–1648.
[19] D.Z. Ni, L. Wang, Y.H. Sun, Z.R. Guan, S. Yang, K.B. Zhou, Amphiphilic hollow carbonaceous microspheres with permeable shells, Angew. Chem.: Int. Ed. 49 (2010) 4223–4227.
[20] L. Wang, D.Z. Ni, D. Yang, K.B. Zhou, S. Yang, Single-hole carbonaceous microcapsules, Chem. Lett. 39 (2010) 451–453.
[21] A.M. Carmo, L.S. Hundal, M.L. Thompson, Sorption of hydrophobic organic compounds by soil materials: application of unit equivalent Freundlich coefficients, Environ. Sci. Technol. 34 (2000) 4363–4369.
[22] B.L. Chen, D.D. Zhou, L.Z. Zhu, Transitional adsorption and partition of nonpolar and polar aromatic contaminants by biochars of pine needles with different pyrolytic temperatures, Environ. Sci. Technol. 42 (2008) 5137–5143.
[23] G.F. Liu, J. Ma, X.C. Li, Q.D. Qin, Adsorption of bisphenol A from aqueous solution onto activated carbons with different modification treatments, J. Hazard. Mater. 164 (2009) 1275–1280.
[24] Y.S. Ho, J.C.Y. Ng, G. McKay, Kinetics of pollutant sorption by biosorbents: review, Sep. Purif. Methods 29 (2000) 189–232.
[25] N. Baccile, G. Laurent, F. Babonneau, F. Fayon, M.M. Titirici, M. Antonietti, Structural Characterization of hydrothermal carbon spheres by advanced solid-state MAS C-13 NMR investigations, J. Phys. Chem. C 113 (2009) 9644–9654.
[26] M.M. Titirici, M. Antonietti, N. Baccile, Hydrothermal carbon from biomass: a comparison of the local structure from poly- to monosaccharides and pentoses/hexoses, Green Chem. 10 (2008) 1204–1212.
[27] B.L. Chen, E.J. Johnson, B. Chefetz, L.Z. Zhu, B.S. Xing, Sorption of polar and nonpolar aromatic organic contaminants by plant cuticular materials: role of polarity and accessibility, Environ. Sci. Technol. 39 (2005) 6138–6146.
[28] G. Cornelissen, O. Gustafsson, T.D. Bucheli, M.T.O. Jonker, A.A. Koelmans, P.C.M. Van Noort, Extensive sorption of organic compounds to black carbon, coal, and kerogen in sediments and soils: mechanisms and consequences for distribution, bioaccumulation, and biodegradation, Environ. Sci. Technol. 39 (2005) 6881–6895.
[29] S. Kumar, M. Zafar, J.K. Prajapati, S. Kumar, S. Kannepalli, Modeling studies on simultaneous adsorption of phenol and resorcinol onto granular activated carbon from simulated aqueous solution, J. Hazard. Mater. 185 (2011) 287–294.
[30] K. Laszlo, P. Podkoscielny, A. Dabrowski, Heterogeneity of polymer-based active carbons in adsorption of aqueous solutions of phenol and 2,3,4-trichlorophenol, Langmuir 19 (2003) 5287–5294.
[31] L. Damjanovic, V. Rakic, V. Rac, D. Stosic, A. Auroux, The investigation of phenol removal from aqueous solutions by zeolites as solid adsorbents, J. Hazard. Mater. 184 (2010) 477–484.
[32] D.Q. Zhu, S. Kwon, J.J. Pignatello, Adsorption of single-ring organic compounds to wood charcoals prepared under different thermochemical conditions, Environ. Sci. Technol. 39 (2005) 3990–3998.
[33] Y. Chun, G.Y. Sheng, C.T. Chiou, B.S. Xing, Compositions and sorptive properties of crop residue-derived chars, Environ. Sci. Technol. 38 (2004) 4649–4655.
[34] C.T. Chiou, D.E. Kile, Deviations from sorption linearity on soils of polar and nonpolar organic compounds at low relative concentrations, Environ. Sci. Technol. 32 (1998) 338–343.
[35] Y.N. Yang, G.Y. Sheng, Enhanced pesticide sorption by soils containing particulate matter from crop residue burns, Environ. Sci. Technol. 37 (2003) 3635–3639.
[36] B. Chefetz, A.P. Deshmukh, P.G. Hatcher, E.A. Guthrie, Pyrene sorption by natural organic matter, Environ. Sci. Technol. 34 (2000) 2925–2930.
[37] F.C. Spurlock, J.W. Biggar, Thermodynamics of organic-chemical partition in soils. 2. Nonlinear partition of substituted phenylureas from aqueous-solution, Environ. Sci. Technol. 28 (1994) 996–1002.
[38] E.L. Difilippo, R.P. Eganhouse, Assessment of PDMS–water partition coefficients: implications for passive environmental sampling of hydrophobic organic compounds, Environ. Sci. Technol. 44 (2010) 6917–6925.
[39] Y. Chen, J. Pawliszyn, Kinetics and the on-site application of standards in a solid-phase microextraction fiber, Anal. Chem. 76 (2004) 5807–5815.
[40] B. Muijs, M.T.O. Jonker, Temperature-dependent bioaccumulation of polycyclic aromatic hydrocarbons, Environ. Sci. Technol. 43 (2009) 4517–4523.
[41] A. DeryloMarczewska, A.W. Marczewski, A general model for adsorption of organic solutes from dilute aqueous solutions on heterogeneous solids: application for prediction of multisolute adsorption, Langmuir 13 (1997) 1245–1250.
[42] M.C. Burleigh, M.A. Markowitz, M.S. Spector, B.P. Gaber, Porous polysilsesquioxanes for the adsorption of phenols, Environ. Sci. Technol. 36 (2002) 2515–2518.